

Comparative Study of the Grid Current Harmonic Attenuation in a Photovoltaic Generator Due to the Influence of the Synchronization Strategy

Original Scientific Paper

N.F. Guerrero-Rodríguez*

Pontificia Universidad Católica Madre y Maestra
PUCMM, Engineering Sciences
Av. Abraham Lincoln Esq. Romulo Betancourt,
2748, Santo Domingo, Dominican Republic,
nf.guerrero@ce.pucmm.edu.do

F.A. Ramírez-Rivera

Pontificia Universidad Católica Madre y Maestra
PUCMM, Engineering Sciences
Av. Abraham Lincoln Esq. Romulo Betancourt,
2748, Santo Domingo, Dominican Republic,
franciscoramirez@pucmm.edu.do

R.O. Batista-Jorge

Pontificia Universidad Católica Madre y Maestra
PUCMM, Engineering Sciences
Av. Abraham Lincoln Esq. Romulo Betancourt,
2748, Santo Domingo, Dominican Republic,
r.batista@ce.pucmm.edu.do

*Corresponding author

Julio A. Ferreira

Pontificia Universidad Católica Madre y Maestra
PUCMM, Engineering Sciences
Av. Abraham Lincoln Esq. Romulo Betancourt,
2748, Santo Domingo, Dominican Republic,
julioferreira@pucmm.edu.do

Robert Mercado-Ravelo

Pontificia Universidad Católica Madre y Maestra
PUCMM, Engineering Sciences
Av. Abraham Lincoln Esq. Romulo Betancourt,
2748, Santo Domingo, Dominican Republic,
rxmr0001@ce.pucmm.edu.do

Abstract – The present paper studies the current harmonic attenuation for four synchronization strategies commonly used in inverters for photovoltaic power generation. In a model of a 6kWp photovoltaic generator, the four synchronization strategies are implemented in the inverter controller. Real-time simulations are performed, for this purpose, the models of the photovoltaic generator and the utility grid were embedded in an OPAL-RT OP5707XG simulator. The distortion of the grid current for each synchronization strategy is analyzed using its corresponding frequency spectrum and a comparison is made with the IEEE Std. 519-2022 standard. The purpose of this test is to observe the effect of the synchronization strategy on the harmonic attenuation of the grid currents. The results show that one of the synchronization strategies evaluated in this work may be sufficient for the system to comply with the harmonic standard for photovoltaic generators without the use of harmonic compensation structures or active harmonic filters. The evaluation of the harmonic distortion behavior of photovoltaic generators as a function of the synchronization strategy used in the inverter controller is the principal work contribution.

Keywords: Synchronization Strategy, Grid-Connected Photovoltaic Generator, Harmonic Distortion, Inverter, Real-Time Digital Simulator

Received: July 11, 2024; Received in revised form: January 9, 2025; Accepted: January 10, 2025

1. INTRODUCTION

The large number of renewable energy resources (RES) that are integrated into the electrical power distribution system presents several issues, such as harmonic distortion in the utility grid [1-3]. Research has shown that the presence of diode rectifier-based systems and other nonlinear loads adversely affects the power qual-

ity of power systems, mainly due to the harmonic distortion generated by these types of systems [4-6].

Grid voltages are measured in grid-connected photovoltaic (PV) generators and sent to the control system of the inverters that act as power conditioners. These voltages are used in the control block as the synchronization strategy for determining grid parameters like grid

phase angle and grid frequency, and to perform operations such as applying the Park transformations, a PQ power control, among other control techniques applied to these renewable agents. If the grid voltages are affected by harmonic distortions, these harmonics can be introduced into the inverter control system [7], so that the grid currents injected by the PV system contain harmonics coming from the grid voltages [8]. According to [7], if there is harmonic pollution in the grid voltage, the output current will also be affected by the harmonic.

Because the incidence of harmonics can influence the level of quality of the energy injected by photovoltaic generators [5, 9], and the fact that the grid currents must fulfil some normative regarding the harmonic distortion, where a 5% of the Total Harmonic Distortion of current (THD_i) it is recommended [10], several works investigate solutions to the problems due to the grid harmonic distortion caused by non-linear loads.

In [2] the authors examine the effect of grid voltage harmonics on the performance of rectified power converters by formulating the voltage and current harmonics of the converter. A method for finding the inverter current harmonics caused by the PWM signal as a dependence of the load profile is presented by the authors in [3]. In [11], an innovative design method for a Proportional Resonant (PR) controller with a selective harmonic cancellation is described for a grid-connected PV generator.

An integrated approach for improved grid current harmonic compensation including power ripple attenuation in a PV generator is proposed in [12]. In [13, 14], harmonic compensation structures are used to reduce current harmonic levels. Active harmonic filters are also used for this purpose, but there are no feasible for small grid-connected renewable energy system [5].

Previous works had focused on the effect and the techniques needed for harmonics compensation [6], arguments in favor of the need for the application of techniques for the reduction of the presence of harmonics in electrical power distribution systems with a strong presence of RES.

In addition, as can be seen in [15], the harmonics introduced by Inverter-Based Resources (IBR) under a high penetration of RES can, under certain circumstances, impact the system stability.

The ability of a PV inverter to attenuate harmonic currents due to the influenced of the synchronization strategy used in the inverters of photovoltaic generators is analyzed in [16], where the results showed that the synchronization strategy affects the harmonic attenuation capability of the inverter.

Due to the above, the impact of the synchronization strategy on reducing the harmonic distortion in grid-connected PV generators, is analyzed in this work to show their impact in the grid current harmonic attenuation of PV generators when voltage harmonics affect the utility grid.

To carry out the above mentioned, four synchronization strategies will be implemented in the MATLAB/SIMULINK R2022a software [17]. All of them will be simulated in an OPAL-RT's OP5707XG simulator [18] and their behavior will be compared to each other to have a clear analysis of their effect on the grid current harmonic attenuation. For this, the harmonic attenuation of the utility grid current due to the applied synchronization strategies will be analyzed using the corresponding frequency spectrum, and a comparison with the standard IEEE Std. 519-2022 [10] will be made.

The current work is organized in 6 sections: Section 2 provides a brief description of the synchronization strategies that will be evaluated in this work. Section 3 describes a PV generator which will be used as a case study to evaluate the impact that synchronization strategies have on the attenuation of harmonics in the grid currents. The methodology used in this work is shown in Section 4. In Section 5, simulations using MATLAB/SIMULINK R2022a software [17] and an OPAL-RT's OP5707XG simulator [18] are carried out. In Section 6 of this work, the results obtained are discussed and the conclusions are presented.

2. SYNCHRONIZATION STRATEGIES

To properly match the grid currents of the PV inverter to the grid voltages, it is needed to determine the phase angle of the grid [19-21]. A summary description of four synchronization strategies to be used in this comparative study is shown in Table 1.

Fig. 1a displays the diagram of the synchronization strategy named Phase-Locked Loop (PLL), which consists of the Clarke and Park transformations, a PI regulator and a voltage-controlled oscillator [22-24]. Fig. 1b shows the PSD+dqPLL synchronization strategy [22, 25], which consists of a PLL plus a Positive Sequence Detector (PSD) block able of determining the positive sequence of unbalanced grid voltages.

A Dual Second Order Generalized Integrator Frequency-Locked Loop (DSOGI-FLL) [24] synchronization strategy is shown in Fig. 1c, which consists of a block where the Clark transform is applied to the grid voltages, two blocks Quadrature Signal Generation (SOGI-QSG), a Positive Sequence Calculator (PSC) and a Frequency-Locked Loop (FLL).

Fig. 1d shows a Multiple Second Order Generalized Integrator Frequency-Locked Loop (MSOGI-FLL) synchronization strategy, which consists of a Harmonic Decoupling Network (HDN) block used to reject the influence of any other harmonics in the selected harmonic, four SOGI-QSG blocks (for the 1st, 2nd, 5th and 7th harmonics), and a FLL block [26].

Since this work does not aim at a detailed study of each of these algorithms, Table 1 includes references of these algorithms, therefore that interested readers can study its design and operation in detail.

Table 1. Description of the synchronization strategies evaluated in this study

Reference	Name	Acronym	Locked methodology	Digital Filter used	Transfer function
[22-24]	Synchronous Reference Frame Phase-Locked Loop	dqPLL	Phase	Proportional Integrator (PI)	$H(S)=(Kps+Ki)/(s^2+Kps+Ki)$ (1)
[16, 22, 25]	Positive Sequence Detector plus a dqPLL	PSD+dqPLL	Phase	Proportional Integrator (PI)	$H(S)=(Kps+Ki)/(s^2+Kps+Ki)$ (1)
[24]	Dual Second Order Generalized Integrator Frequency-Locked Loop	DSOGI-FLL	Frequency	Second Order Generalized (SOGI)	$SOGI(s)=v'/(kE_v)(s)=\omega's/(s^2+\omega'^2)$ (2)
[26]	Multiple Second Order Generalized Integrator Frequency-Locked Lop	MSOGI-FLL	Frequency	Second Order Generalized (SOGI)	$SOGI(s)=v'/(kE_v)(s)=\omega's/(s^2+\omega'^2)$ (2)

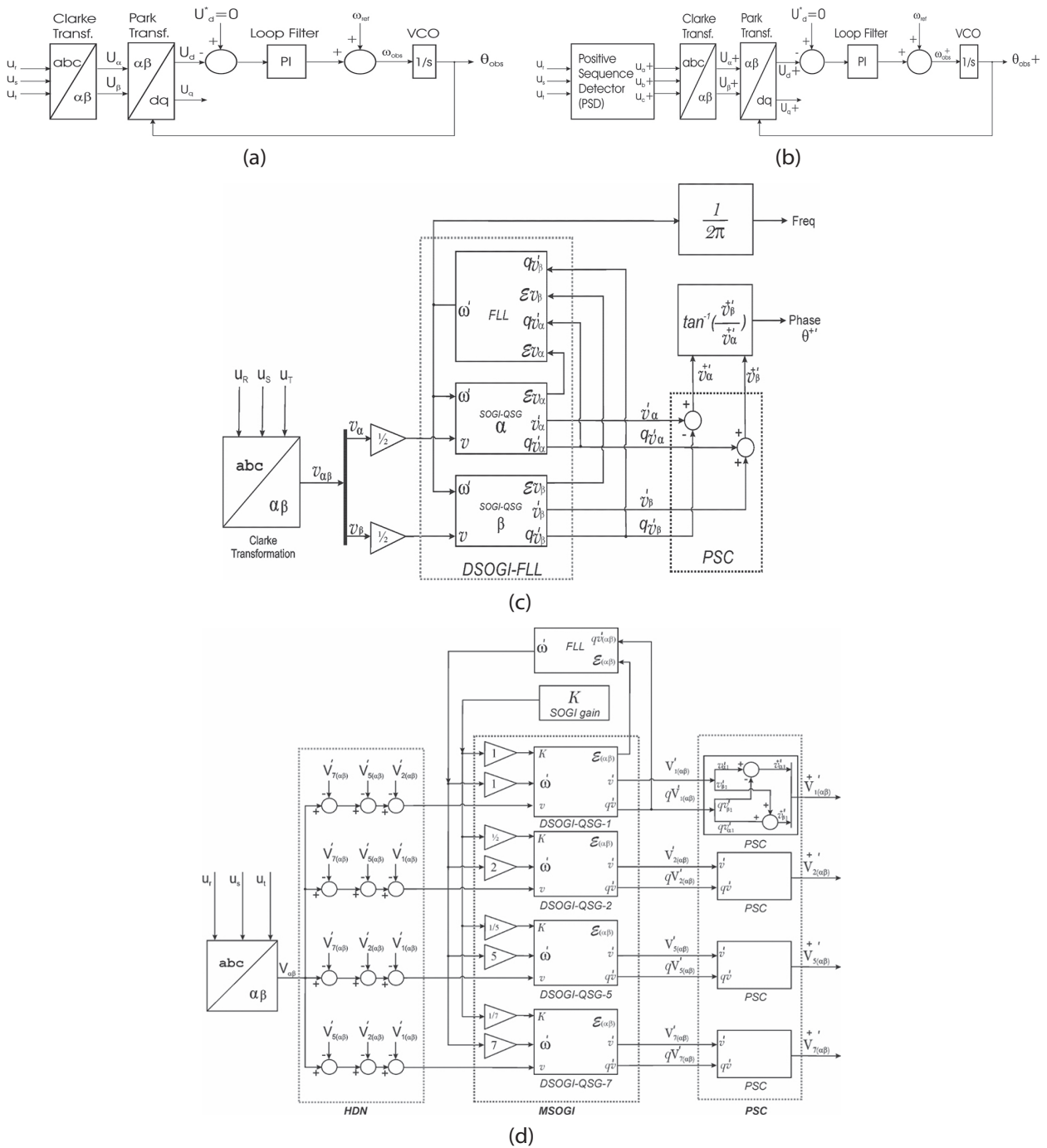


Fig. 1. Block diagrams of the synchronization strategies used in this study [27]. (a) dqPLL. (b) PSD+dqPLL. (c) DSOGI-FLL. (d) MSOGI-FLL

3. PHOTOVOLTAIC GENERATOR FOR CASE STUDY

A 6kWp PV 3-phase grid-connected generator model is used to evaluate the achieved grid current harmonic attenuation for each synchronization strategy analyzed, which is composed of two subsystems, Power and Control. The PV modules [28], the capacitor link, the inverter [29], the LCL filter [30], a transformer [31], an EMI filter [32], and finally, the utility grid [33] form the power subsystem. A maximum power point tracker (MPPT) block [28], [34], a cascade control [35] and the synchronization strategy form the control subsystem.

Table 2 summarized the Power subsystem parameters. The parameters used to design the synchronization strategies are shown in Table 3.

4. METHODOLOGY

Fig. 2 shows a flowchart of the methodology used in this work. A MATLAB/SIMULINK model of a 6kWp PV generator is developed using the parameters shown in Tables 2 and 3, implementing the synchronization strategies shown in Section 2. After validating the correct functioning of the MATLAB/SIMULINK model, the distortion caused by non-linear loads and converters used by renewable energy sources is simulated by voltage harmonics introduced into the 3-phase low-voltage utility grid. For this purpose, a 4% harmonic contamination in the 5th and 7th harmonics in the grid voltages is applied, attaining a Total Harmonic Distortion of voltage (THD_v) of 5.66%. For modelling the voltage grid with harmonic distortion, the system voltage of Eq. (3) is used.

$$\begin{aligned}
 U_{gr}(t) &= U_{1r} \cos(\omega t + \theta_{U1r}) \\
 &\quad + U_{h5r} \cos(5\omega t + \theta_{Uh5r}) \\
 &\quad + U_{h7r} \cos(7\omega t + \theta_{Uh7r}) \\
 U_{gs}(t) &= U_{1s} \cos(\omega t + \theta_{U1s}) \\
 &\quad + U_{h5s} \cos(5\omega t + \theta_{Uh5s}) \\
 &\quad + U_{h7s} \cos(7\omega t + \theta_{Uh7s}) \\
 U_{gt}(t) &= U_{1t} \cos(\omega t + \theta_{U1t}) \\
 &\quad + U_{h5t} \cos(5\omega t + \theta_{Uh5t}) \\
 &\quad + U_{h7t} \cos(7\omega t + \theta_{Uh7t})
 \end{aligned} \quad (3)$$

where h is the harmonic order, ω is the angular fundamental frequency, U is the voltage magnitude, θ is the voltage phase angle of the fundamental frequency, and θ_{Uh} is the voltage phase angle of the harmonic h .

Table 2. PV power subsystem parameters

Parameters	Value
Utility grid	$V_{rms}=220V$ (ph-ph), 50Hz
Utility grid Total Harmonic Distortion of voltage	$THD_v=5.66\%$
Outer Filter	$R=20$ mΩ, $C=1.5$ μF, $L=3.9$ mH
Transformer	50Hz, 308/232V, $S_{nom}=6$ kVA
Voltage Source Inverter	SKS22FB6U+E1CIF+B6CI, SEMISTACK-IGBT
DC bus voltage	$V_{cc}=350$ V
PV power	$P=6$ kW

The synchronization strategies evaluated must be able to identify the frequency and phase of the 3-phase grid voltages in the presence of harmonic distortion, so that this information is sent to the PV generator control system to ensure proper inverter operation. If the phase and frequency of the grid are not detected during the MATLAB/SIMULINK simulations, it will be necessary to readjust the parameters governing the response and stability of the synchronization strategies studied, which are shown in Table 3.

After evaluating the operation of the photovoltaic generator in the presence of voltage harmonics, experiments will be performed using a real-time digital simulator. This allows tests to be carried out with certain similarities to those of a physical photovoltaic system.

The harmonic distortion of the utility grid current for each synchronization strategy is analyzed using its corresponding frequency spectrum and a comparison is made with the standard IEEE Std. 519-2022.

Table 3. Parameters of the synchronization strategies

Parameters	Value
PLL natural angular frequency	130 rad/s
Settling time	50 ms
Damping factor for the dqPLL	$\sqrt{2}/2$
Gain of the SOGI	$\sqrt{2}$
Damping factor for the DSOGI	0.707
Centre angular frequency for the DSOGI	314 rad/s
Gain to the settling time of the FLL block	100

The above is done to observe the impact of the synchronization strategies into harmonic attenuation of the currents. A calculation of the THD_i of the inverter grid currents is carried out for each synchronization strategy used, then the results obtained are compared and discussed.

The THD_i of the grid current is determined using the synchronization strategies shown in Table 1. The THD_i can be calculated using Eq. (4) [36].

$$THD_i (\%) = \frac{\sqrt{[(I_2)^2 + (I_3)^2 + (I_4)^2 + (I_5)^2 + (I_n)^2]}}{I_1} \times 100 \quad (4)$$

where I_n and I_1 are the individual harmonic current distortion values in amperes and the fundamental current distortion values in amperes, respectively.

5. RESULTS

5.1. MATLAB SIMULATIONS

Modeling is done in MATLAB/SIMULINK2022a software [17] using the synchronization strategies shown in Table 1 and the values from Table 2 and Table 3. As a result of the MATLAB/SIMULINK simulations, Fig. 3a shows the grid voltages disturbed by a THD_v of 5.66%. The deformation of the 3-phase grid voltages due to the

5th and 7th harmonics can be observed. The distortion is intentionally added to the utility grid so that when these harmonics are sensed for feedback to the PV generator control subsystem, they interfere with the control subsystem. When the grid voltage signals are sent, the ability to identify the frequency and phase of the grid could

be affected. This will allow the effect of synchronization strategies to cancel current harmonics at the inverter output when the grid is affected by voltage harmonics.

Because of harmonic distortion in the grid voltages, Fig.3b-c show the detected angular frequencies and phases by the synchronization strategies.

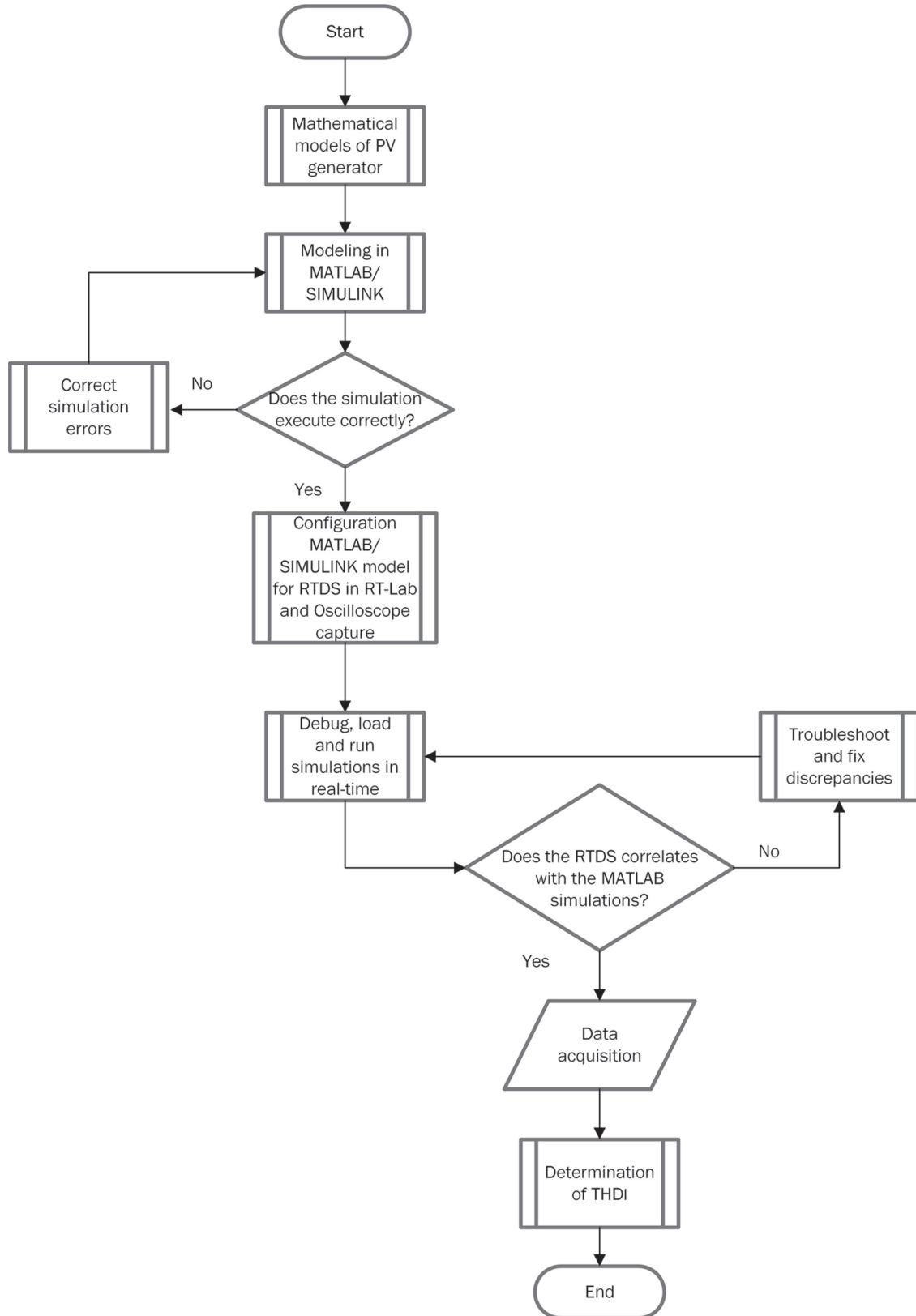


Fig. 2. Flowchart of the methodology to be used

Fig. 3b shows significant oscillations in the frequencies estimated by dqPLL and PSD+dqPLL (red and black, respectively), demonstrating the poor ability of these synchronization strategies to detect the grid frequency under conditions of harmonic distortion. In blue of Fig. 3b, a smaller oscillation is observed in the frequency detected by DSOGI-FLL, which allows a more approximate estimation of the grid frequency with respect to the frequencies obtained by dqPLL and PSD+dqPLL synchronization strategies. A better detection of the frequency is done by

the MSOGI-FLL, as can be observed in yellow. This allows the control signals obtained from the synchronization strategy are not affected by the harmonic distortion of the grid voltages shown in Fig. 3a. As shown in Fig. 3c, poor phase detection is seen with dqPLL (red) and PSD+dqPLL (black); this is mainly due to the setting of the natural angular frequency of the PI regulator, which requires a trade-off between good harmonic attenuation and high dynamics. As shown in Fig.3c (yellow), near perfect phase detection is achieved with the MSOGI-FLL.

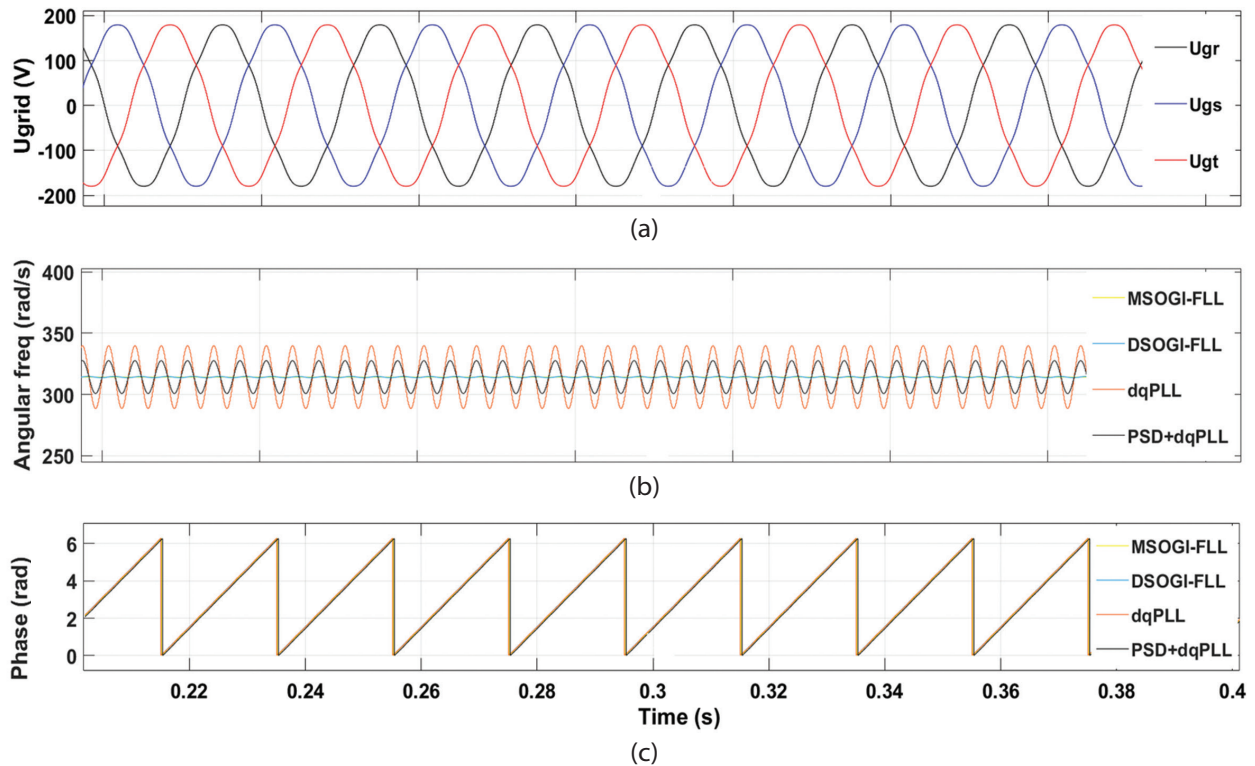


Fig. 3. (a) Grid voltages with harmonic pollution ($THD_v = 5.66\%$). (b) Time evolution of the detected angular frequency by the synchronization strategies under harmonic pollution. (c) Time evolution of the phase detection by the synchronization strategies under harmonic pollution

5.2. REAL-TIME DIGITAL SIMULATIONS

A photograph of the setup used to perform the real-time tests is shown in Fig. 4. It can be seen the OP5707XG real-time simulator, a server as the host PC and lastly, an oscilloscope is employed to record the voltage and current traces. A diagram of the real-time simulation configuration is displayed in Fig. 5 where can be seen the OP5707XG simulator, the Siglent SD-S1204X-E oscilloscope and the PowerEdge R230 server computer host PC [37].

Fig. 6a shows the grid current when a dqPLL was used as the synchronization strategy, where there is significant distortion of the current waveform due to the presence of harmonics. As shown in the frequency spectrum in Fig. 6b, which corresponds to the grid current in Fig. 6a, the 5th and 7th harmonics are present. In percentage terms, the distortion at the 5th and 7th harmonics is 4.66% and 4.73%, respectively.

This results in a THD_i of 6.63%, which is higher than the maximum THD_i of 5% allowed by the IEEE Std. 519-2022 Standard.

The grid current when using a PSD+dqPLL synchronization strategy is shown in Fig. 7a. Comparing the current waveform with that obtained using dqPLL, a slight reduction in the harmonic distortion of the grid current can be observed. In the frequency spectrum in Fig. 7b, which corresponds to the grid current in Fig. 7a, the presence of the 5th and 7th order current harmonics can be observed, with percentages of 3.86% and 3.78% respectively, giving a $THD_i = 5.40\%$. However, despite the significant harmonic attenuation, the results do not comply with the limit proposed by the IEEE Std. 519-2022 Standard.

Fig. 8a shows the grid current using a DSOGI-FLL as a synchronization strategy. There is distortion of the current waveform due to the presence of harmonics. As can be seen from the frequency spectrum in Fig. 8b,

which corresponds to the grid current in Fig. 8a, the 5th and 7th harmonics are present. In percentage terms, the distortion at the 5th and 7th harmonics is 3.69% and 3.67%, respectively. A $THD_i=5.20\%$ of the grid current was achieved, this value being higher than the 5% suggested by the regulations. Regarding the results obtained with the dqPLL and PSD+dqPLL synchronization strategies, significant harmonic attenuation was achieved when DSOGI-FLL was used.

Fig. 9a shows the grid current using a MSOGI-FLL as a synchronization strategy. Note the distortion of the current waveform due to harmonic pollution, how-

ever, when comparing the waveform with the current waveforms using the other synchronization strategies (Fig. 6a, 7a and 8a), the current waveform distortion using MSOGI-FLL is lower. The 5th and 7th harmonics are present in the frequency spectrum in Fig. 9b, which corresponds to the grid current in Fig. 9a. Expressed as a percentage, the 5th and 7th harmonic distortions are 3.15% and 3.36% respectively.

The percentage values for the 5th and 7th harmonics reveal that a significant attenuation of harmonics was achieved, resulting in a THD_i in the grid current of 4.60%, in compliance with the IEEE Std. 519-2022 Standard.



Fig. 4. Photo of the set-up for the execution of the simulations in real-time

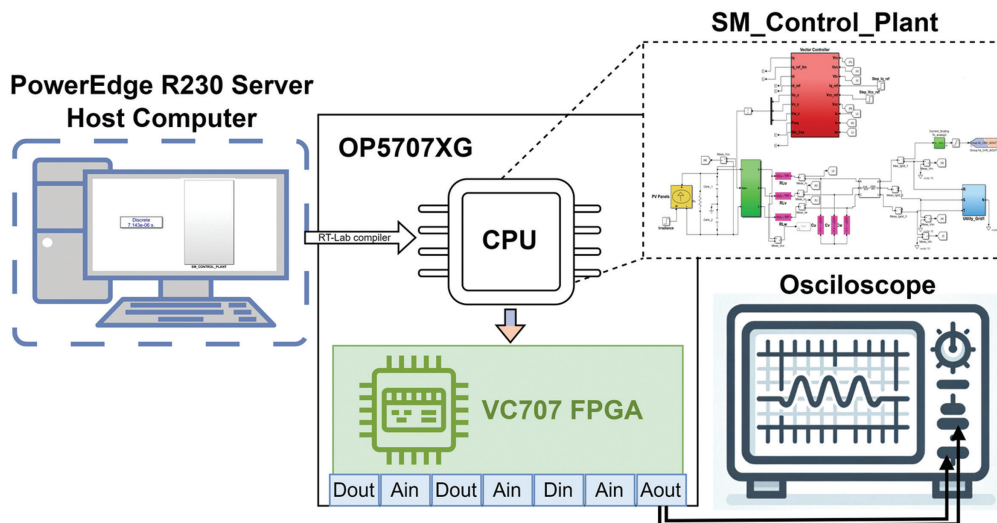
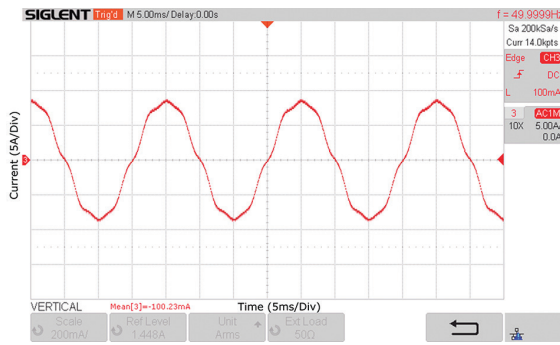


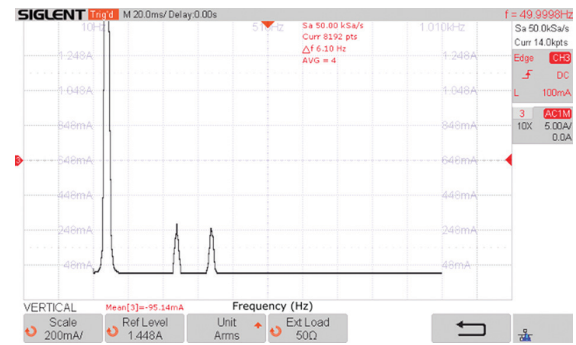
Fig. 5. Block diagram for the configuration of the simulations in real-time

The equivalent amplitude distortion in the grid current at phase 1 for the harmonics is shown in Table 4. Additionally, the resulting harmonic distortion when

each synchronization strategy is applied is shown and compared to the IEEE Std. 519-2022 Standard.

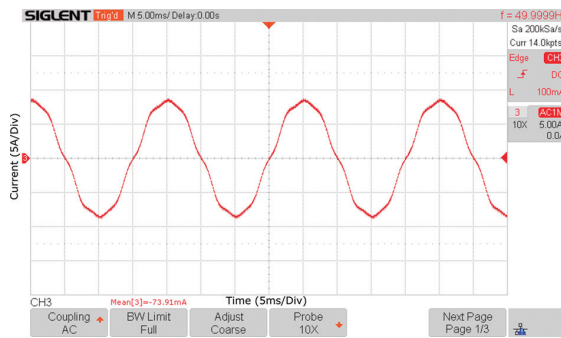


(a)

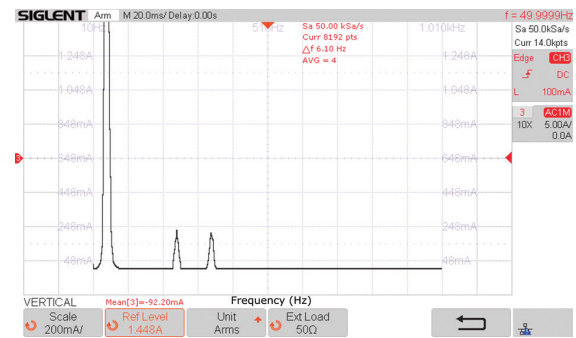


(b)

Fig. 6. (a) Grid current corresponding to phase 1 when using a dqPLL is used. **(b)** Frequency spectrum corresponding to the grid current of phase 1 when a dqPLL is used



(a)

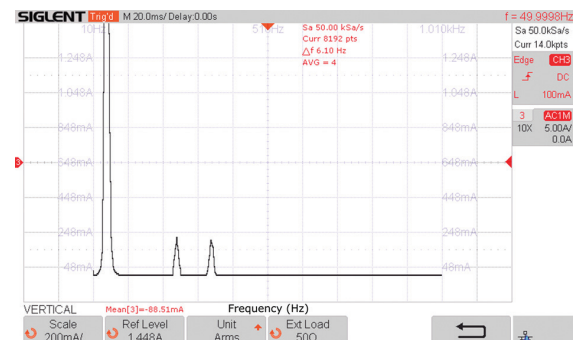


(b)

Fig. 7. (a) Grid current corresponding to phase 1 when a PSD+dqPLL is used. **(b)** Frequency spectrum corresponding to the grid current of phase 1 when a PSD+dqPLL is used

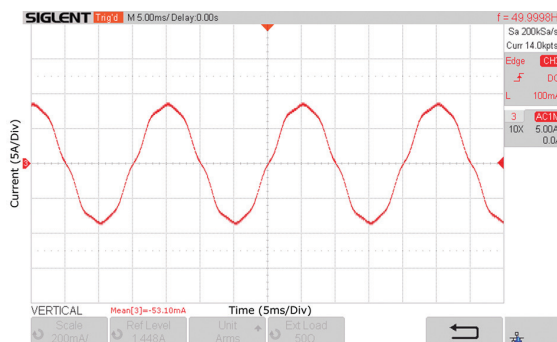


(a)

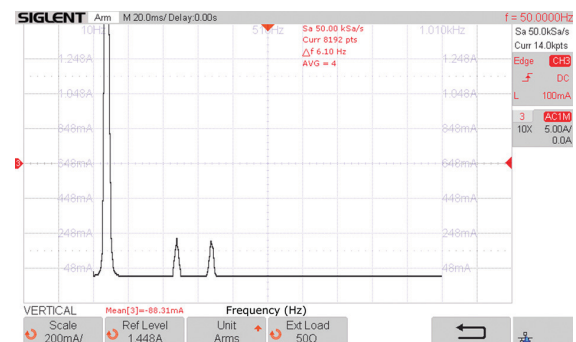


(b)

Fig. 8. (a) Grid current corresponding to phase 1 when a DSOGI-FLL is used. **(b)** Frequency spectrum corresponding to the grid current of phase 1 when a DSOGI-FLL is used



(a)



(b)

Fig. 9. (a) Grid current corresponding to phase 1 when a MSOGI-FLL is used. **(b)** Frequency spectrum corresponding to the grid current of phase 1 when a MSOGI-FLL is used

Table 4. Harmonic distortion corresponding to the grid current of phase 1

Name	5 th Harmonic distortion (%)	7 th Harmonic distortion (%)	Distortion limit (%)	THD_i (%)	THD_i limit (%)
dqPLL	4.66	4.73	< 4.0	6.63	< 5.0
PSD+dqPLL	3.86	3.78	< 4.0	5.40	< 5.0
DSOGI-FLL	3.69	3.67	< 4.0	5.20	< 5.0
MSOGI-FLL	3.15	3.36	< 4.0	4.60	< 5.0

6. DISCUSSION AND CONCLUSION

Table 4 shows a summary of the THD_i of the grid current resulting from using the synchronization strategies shown in Table 1. Furthermore, these resulting THD_i values are evaluated with the IEEE Std. 519-2022 Standard. On the one hand, significant harmonic attenuation is observed when the MSOGI-FLL synchronization strategy is used. On the other hand, a poor harmonic attenuation is obtained when the dqPLL synchronization strategy was employed.

The contribution of four synchronization strategies to decrease the magnitude of current harmonics in PV generators when the grid voltage is disturbed by harmonic pollution was studied in this paper. Following, a resume of the performances of these synchronization strategies are remarked:

The dqPLL synchronization strategy uses a PI which behaves as a low pass filter. However, for the settling time used along the paper, the cutoff frequency is not enough to attenuate properly the harmonics, and, consequently, a poor harmonic attenuation is attained.

Compared to dqPLL, the notable attenuation of harmonic distortion achieved when using the PSD+dqPLL is due to the use of the positive sequence detector (PSD) block which cancels the effect of the negative sequence of the 5th harmonic. The above allows better detection of the grid phase and grid frequency, thus sending reliable information to the inverter controller used in the PV generator.

When the DSOGI-FLL is compared with the dqPLL, a greater reduction of harmonic contamination was obtained using the DSOGI-FLL. This better behavior is because a Positive Sequence Calculator block is used in the DSOGI-FLL. Despite the harmonic attenuation achieved, a significant harmonic contamination can be observed in the grid current, and then, the obtained THD_i exceeds the limits imposed by the standard on grid current harmonics IEEE Std. 519-2022.

When the MSOGI-FLL was tested, an important rejection in the harmonic distortion of the grid current harmonic was observed due to the use of the block Harmonic Decoupled Network [26], in addition to a DSOGI block corresponding to each of the harmonics found in the utility grid. Also, several Positive Sequence Calculator blocks were implemented, to attain only the positive sequence of the harmonic of the grid voltages and, as consequence, rejecting the harmonic pollution effects of the negative sequence.

This work concludes that depending on the synchronization strategy used, a different behavior of harmonic distortion attenuation is observed in the grid currents of photovoltaic generators. MSOGI-FLL is an effective solution to reject the magnitude certain number of harmonics.

ACKNOWLEDGMENTS:

This research was funded by the MESCyT (Ministry of Higher Education Science and Technology) in the Dominican Republic through Fondocyt, under the projects Development of New Methodologies for Harmonic Mitigation in Grid-connected Electrical Power Systems (2020-2021-3A9-068) and, Development of Methodologies Based on Solar-photovoltaic Green Hydrogen to Stabilize the Electrical Grid and Reduce the Carbon Footprint for Electrical Generation (2022-3C1-168).

7. REFERENCES:

- [1] A. Alduraibi, "Analysis of harmonics generated by power converters in power networks: impacts and mitigation techniques", School of Information Technology and Electrical Engineering, The University of Queensland, 2021, PhD Thesis.
- [2] A. Alduraibi, J. Yaghoobi, F. Zare, "Impacts of Grid Voltage Harmonics Amplitude and Phase Angle Values on Power Converters in Distribution Networks", IEEE Access, Vol. 9, 2021, pp. 92017-92029.
- [3] J. Yaghoobi, F. Zare, "Impacts of three-phase power converter operating modes on harmonic emissions in distribution networks: Harmonics emission within 2-9 kHz", IET Power Electronics, Vol. 13, No. 13, 2020, pp. 2935-2942.
- [4] J. Yaghoobi, A. Alduraibi, D. Martin, F. Zare, D. Eghbal, R. Memisevic, "Impact of high-frequency harmonics (0-9 kHz) generated by grid-connected inverters on distribution transformers", International Journal of Electrical Power and Energy Systems, Vol. 122, 2020, p. 106177.
- [5] R. Ekström, M. Leijon, "Lower order grid current harmonics for a voltage-source inverter connected to a distorted grid", Electric Power Systems Research, Vol. 106, 2014, pp. 226-231.

- [6] A. Kalair, N. Abas, A. R. Kalair, Z. Saleem, N. Khan, "Review of harmonic analysis, modeling and mitigation techniques", *Renewable and Sustainable Energy Reviews*, Vol. 78, 2017, pp. 1152-1187.
- [7] Y. Du, D. D. C. Lu, G. James, D. J. Cornforth, "Modeling and analysis of current harmonic distortion from grid connected PV inverters under different operating conditions", *Solar Energy*, Vol. 94, 2013, pp. 182-194.
- [8] N. F. Guerrero-Rodríguez, A. B. Rey-Boué, "Modeling, simulation and experimental verification for renewable agents connected to a distorted utility grid using a Real-Time Digital Simulation Platform", *Energy Convers Manag*, Vol. 84, 2014, pp. 108-121.
- [9] J. Badugu, Y. P. Obulesu, C. S. Babu, "Investigation of THD Analysis in Residential Distribution Systems with Different Penetration Levels of Electric Vehicles", *International Journal of Electrical and Computer Engineering Systems*, Vol. 9, No. 1, 2018, pp. 21-27.
- [10] Institute of Electrical and Electronics Engineers IEEE, "519-2022 - IEEE Standard for Harmonic Control in Electric Power Systems", 2022.
- [11] C. Yanarates, Z. Zhou, "Symmetrical Pole Placement Method-Based Unity Proportional Gain Resonant and Gain Scheduled Proportional (PR-P) Controller with Harmonic Compensator for Single Phase Grid-Connected PV Inverters", *IEEE Access*, Vol. 9, 2021, pp. 93165-93181.
- [12] M. Mishra, V. N. Lal, "An Advanced Proportional Multiresonant Controller for Enhanced Harmonic Compensation with Power Ripple Mitigation of Grid-Integrated PV Systems under Distorted Grid Voltage Conditions", *IEEE Transactions on Industry Applications*, Vol. 57, No. 5, 2021, pp. 5318-5331.
- [13] L. S. Xavier, A. F. Cupertino, J. T. de Resende, V. F. Mendes, H. A. Pereira, "Adaptive current control strategy for harmonic compensation in single-phase solar inverters", *Electric Power Systems Research*, Vol. 142, 2017, pp. 84-95.
- [14] D. Zammit, C. S. Staines, M. Apap, J. Licari, "Design of PR current control with selective harmonic compensators using Matlab", *Journal of Electrical Systems and Information Technology*, Vol. 4, No. 3, 2017, pp. 347-358.
- [15] Z. Deng, G. Todeschini, "A Novel Approach for Harmonic Assessment of Power Systems With Large Penetration of IBRs - A U.K. Case Study", *IEEE Transactions on Power Delivery*, Vol. 39, No. 1, 2024, pp. 455-466.
- [16] N. F. Guerrero-Rodríguez, L. C. Herrero-de Lucas, S. de Pablo-Gómez, A. B. Rey-Boué, "Performance study of a synchronization algorithm for a 3-phase photovoltaic grid-connected system under harmonic distortions and unbalances", *Electric Power Systems Research*, Vol. 116, 2014, pp. 252-265.
- [17] MathWorks, "MATLAB/SIMULINK", <https://www.mathworks.com/products/matlab.html> (accessed: 2024)
- [18] OPAL-RT, "POWER HARDWARE-IN-THE -LOOP", <https://www.opal-rt.com/power-hardware-in-the-loop/> (accessed: 2024)
- [19] W. A. Sotelo, D. J. Rincon, M. A. Mantilla, J. M. Rey, Z. Zheng, "Performance Analysis of Three-Phase Synchronization Algorithms Under Voltage Sags", *Proceedings of IECON 2022 - 48th Annual Conference of the IEEE Industrial Electronics Society*, Brussels, Belgium, 17-20 October 2022, pp. 1-6.
- [20] F. Blaabjerg, R. Teodorescu, M. Liserre, A. V Timbus, "Overview of control and grid synchronization for distributed power generation systems", *IEEE Transactions on Industrial Electronics*, Vol. 53, No. 5, 2006, pp. 1398-1409.
- [21] S. V. Kulkarni, D. N. Gaonkar, "An investigation of PLL synchronization techniques for distributed generation sources in the grid-connected mode of operation", *Electric Power Systems Research*, Vol. 223, 2023, p. 109535.
- [22] M. Karimi-Ghartemani, M. R. Iravani, "A Method for Synchronization of Power Electronic Converters in Polluted and Variable-Frequency Environments", *IEEE Transactions on Power Systems*, Vol. 19, No. 3, 2004, pp. 1263-1270.
- [23] R. Teodorescu, M. Liserre, P. Rodriguez, "Grid Converters for Photovoltaic and Wind Power Systems", John Wiley & Sons, 2011.
- [24] P. Rodríguez, R. Teodorescu, I. Candela, A. V. Timbus, M. Liserre, F. Blaabjerg, "New positive-sequence voltage detector for grid synchronization

- of power converters under faulty grid conditions”, Proceedings of the 37th IEEE Power Electronics Specialists Conference, Jeju, Korea, 18-22 June 2006, pp. 1-7.
- [25] C. L. Fortescue, “Method of Symmetrical Co-Ordinates Applied to the Solution of Polyphase Networks”, Transactions of the American Institute of Electrical Engineers, Vol. XXXVII, No. 2, 1918, pp. 1027-1140.
- [26] P. Rodriguez, A. Luna, I. Candela, R. Mujal, R. Teodorescu, F. Blaabjerg, “Multiresonant Frequency-Locked Loop for Grid Synchronization of Power Converters Under Distorted Grid Conditions”, IEEE Transactions on Industrial Electronics, Vol. 58, No. 1, 2011, pp. 127-138.
- [27] N. F. Guerrero-Rodríguez, A. B. Rey-Boué, E. J. Bueno, O. Ortiz, E. Reyes-Archundia, “Synchronization algorithms for grid-connected renewable systems: Overview, tests and comparative analysis”, Renewable and Sustainable Energy Reviews, Vol. 75, 2017, pp. 629-643.
- [28] P. V. Mahesh, S. Meyyappan, R. Alla, “Support Vector Regression Machine Learning based Maximum Power Point Tracking for Solar Photovoltaic systems”, International Journal of Electrical and Computer Engineering Systems, Vol. 14, No. 1, 2023, pp. 100-108.
- [29] S. A. Zulkifli, E. Y. Riyandra, S. Salimin, A. N. Zaidan, R. Jackson, “Investigation of Multilevel Inverter for the Next Distributed Generation Using Low-Cost Microcontroller”, International Journal of Electrical and Computer Engineering Systems, Vol. 10, No. 1, 2019, pp. 11-18.
- [30] M. T. Faiz et al. “An alternative control synthesis for stability enhancement of digital-controlled LCL-filtered grid-connected inverter”, Electric Power Systems Research, Vol. 213, 2022, p. 108678.
- [31] L. Zhang et al. “Collaborative optimization control of hybrid distribution transformers integrated with photovoltaics in unbalanced distribution networks”, International Journal of Electrical Power & Energy Systems, Vol. 159, 2024, p. 110052.
- [32] L. Sandrolini, A. Mariscotti, “Impact of short-time fourier transform parameters on the accuracy of EMI spectra estimates in the 2-150 kHz supraharmmonic interval”, Electric Power Systems Research, Vol. 195, 2021, p. 107130.
- [33] T. Y et al. “Optimization of Distributed Generation in Radial Distribution Network for Active Power Loss Minimization using Jellyfish Search Optimizer Algorithm”, International Journal of Electrical and Computer Engineering Systems, Vol. 15, No. 3, 2024, pp. 215-223.
- [34] M. Oubella, M. Ajaamoum, B. Bouachrine, “Low cost microcontroller implementation of Takagi-Sugeno Fuzzy MPPT controller for photovoltaic systems”, International Journal of Electrical and Computer Engineering Systems, Vol. 13, No. 10, 2022, pp. 971-981.
- [35] S. Buso, P. Mattavelli, “Digital Control in Power Electronics”, Morgan & Claypool Publishers, 2006.
- [36] M. Turarbek, A. Ruderman, B. Reznikov, “Calculation of Current Total Harmonic Distortion for a Single-Phase Current Source Multilevel Inverter”, Proceedings of the IEEE 14th International Conference on Compatibility, Power Electronics and Power Engineering, Setubal, Portugal, 8-10 July 2020, pp. 249-254.
- [37] N. F. Guerrero-Rodríguez, R. O. Batista-Jorge, F. A. Ramírez-Rivera, J. Ferreira, R. Mercado-Ravelo, A. Manilla, “Harmonic Distortion Study of a Photovoltaic Generator in a Microgrid under Disturbances”, Energies, Vol. 17, No. 9, 2024, p. 2031.